Single-Molecule Magnets

DFT Computational Rationalization of an Unusual Spin Ground State in an Mn_{12} Single-Molecule Magnet with a Low-Symmetry Loop Structure**

*Dolos Foguet-Albiol, Ted A. O'Brien, Wolfgang Wernsdorfer, Brian Moulton, Michael J. Zaworotko, Khalil A. Abboud, and George Christou**

Single-molecule magnets (SMMs) represent a molecular approach to nanoscale magnetic materials. They are molecules possessing a large barrier (versus kT) to magnetization relaxation, and thus display magnetization versus applied-field hysteresis loops at low enough temperatures, the diagnostic property of a magnet.[1] SMMs derive their properties from a combination of a large ground-state spin (S) value and a significant magnetoanisotropy of the Ising (easy-axis) type.

Deprotonated pyridine-2,6-dimethanol ($pdmH_2$) has proven a versatile N,O,O chelating and bridging ligand in our manganese-cluster chemistry. It has been found as a chelate in species such as $[PtCl_2(pdmH_2)]$,[2] $[TcOCl(pdmH)_2]$,[3] and $[\{MoO_2(pdm)\}_n]$.[4] In manganese chemistry, the alkoxide arms also act as bridging groups yielding polynuclear clusters such as $[Mn_4(O_2CMe)_2(pdmH)_6]^{2+}$ with $S = 9$,[5] $[Mn_9(O_2CEt)_{12}(pdm)(pdmH)_2(L)_2]$ with $S = 11/2$,[6] and $[Mn_{25}O_{18}(OH)_2(N_3)_{12}(pdm)_6(pdmH)_6]^{2+}$ with $S = 51/2$.[7] All these complexes are SMMs. Recently, we have been exploring the products from reactions employing *N*-methyldiethanolamine ($mdaH_2$). This is also a N,O,O chelate, but is more flexible than $pdmH_2$ and we anticipated that it might lead to new types of manganese clusters; we were unaware of any use of $mdaH_2$ in manganese chemistry. We herein report the synthesis and properties of Mn_4 and Mn_{12} clusters with this ligand, and show that they are new SMMs. Further, the Mn_{12} cluster has an unusual ground-state spin value for a loop structure, and we provide rationalization for this using DFT calculations.

The reactions of $mdaH_2$ have been investigated with a variety of Mn carboxylate sources and under a variety of conditions. The reaction between $Mn(O_2CMe)_2{\cdot}4H_2O$, $mdaH_2$,and NEt_3 in a 1:1:1 molar ratio in MeCN resulted in the formation of $[Mn_{12}(O_2CMe)_{14}(mda)_8]{\cdot}MeCN$ (**1**·MeCN) in 55% yield. In contrast, when the same reaction was carried out with the bulkier benzoate group by using $Mn(O_2CPh)_2{\cdot}4H_2O$, the crystalline product was $[Mn_4(O_2CPh)_4(mda)_2(mdaH)_2]{\cdot}CH_2Cl_2{\cdot}Et_2O$ (**2**·CH_2Cl_2·Et_2O) in 16% yield. The crystal structure of complex **1**[8] consists of a Mn_{12} loop with crystallographic *Ci* symmetry that is mixed-valent ($Mn^{II}_6Mn^{III}_6$) and possesses a chair conformation (Figure 1, top). All the manganese centers are six-coordinate except Mn^{II} ions Mn4 and Mn4′, which have a very distorted pentagonal-bipyramidal coordination sphere. Six mda^{2-} ligands each chelate a Mn^{III} ion, and the two alkoxide O atoms bridge to the adjacent Mn^{II} ions. The other two mda^{2-} groups chelate Mn^{II} ions and bridge by their alkoxide O atoms to Mn^{III} ions. As a result, the mda^{2-} groups alternate between being axial and equatorial with respect to

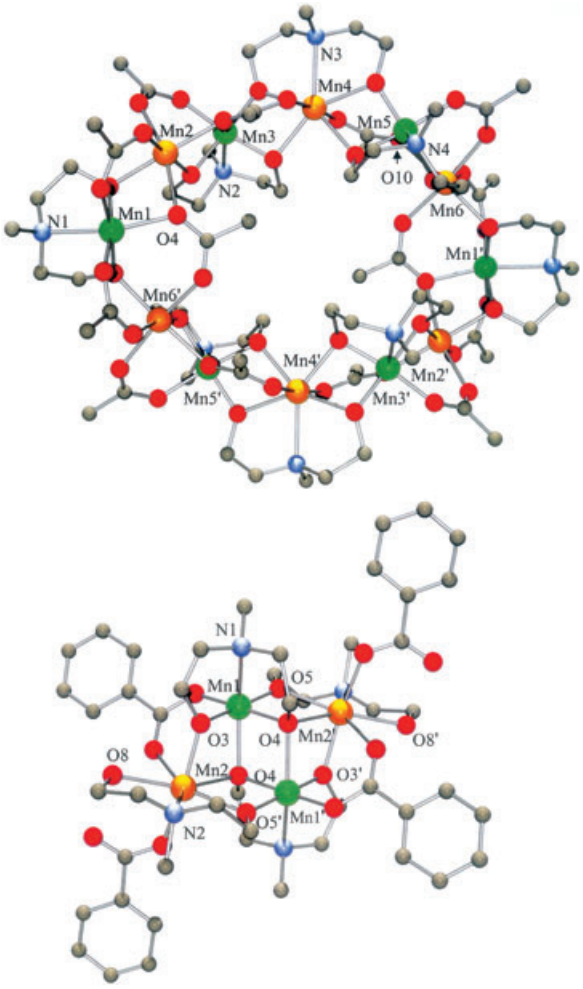

Figure 1. PovRay plot of complexes **1** (top) and **2** (bottom). Color scheme: Mn^{III} green, Mn^{II} orange, O red, N blue, C gray. H atoms have been omitted for clarity.

[*] D. Foguet-Albiol, Dr. K. A. Abboud, Prof. Dr. G. Christou
Department of Chemistry
University of Florida
Gainesville, FL 32611-7200 (USA)
Fax: (+1) 352-392-8757
E-mail: christou@chem.ufl.edu
Dr. W. Wernsdorfer
Laboratoire Louis Néel-CNRS, BP-166
Grenoble, Cedex 9 (France)
Dr. T. A. O'Brien
Department of Chemistry
Indiana University-Purdue University Indianapolis
Indianapolis, IN 46202-3274 (USA)
Dr. B. Moulton, Prof. Dr. M. J. Zaworotko
Department of Chemistry
University of South Florida, Tampa, FL 33620 (USA)

[**] This work was supported by the U.S. National Science Foundation (Grant CHE-0414155).

 DOI: 10.1002/ange.200461820

the plane of the Mn_{12} loop. Each Mn_2 pair is additionally bridged by an acetate group in its familiar η^1,η^1,μ (*syn*,*syn*) binding mode on the outside of the loop, whereas the final two acetate groups bridge in a rarer η^1,η^2,μ_3 mode on the inside of the loop. The Mn^{II}/Mn^{III} oxidation state assignments were established by consideration of bond lengths, bond-valence sum (BVS) calculations[9] and the presence of Jahn–Teller (JT) distortions at six of the Mn ions, as expected for high-spin Mn^{III} in near-octahedral geometry; the JT axes all contain the mda^{2-} N atoms.

The structure of **2**[8] is similar to that of $[Mn_4(O_2C\text{-}Me)_2(pdmH)_6]^{2+}$[5] and consists of a Mn_4 planar rhombus that can be described as two edge-fused Mn_3 triangular units (Figure 1, bottom). Inspection of structural parameters, BVS calculations, and detection of Mn^{III} JT elongation axes at Mn1/Mn1′ identifies Mn1/Mn1′ as Mn^{III} and Mn2/Mn2′ as Mn^{II} centers. Each Mn^{III} ion is chelated by a tridentate mda^{2-} group, one of whose alkoxide O atoms (O3) bridges to Mn2, and the other (O4) to Mn1′ and Mn2′. The two $mdaH^-$ groups also each bind in a tridentate fashion, with one of their alkoxide O atoms (O5) doubly bridging to Mn2′ but the other (O8) being protonated, terminally bound to Mn2, and forming a hydrogen bond to the unbound O atom of the monodentate benzoate ligand. This situation was confirmed by the BVS for O8 being 1.15, as expected for a protonated O atom whose bound H^+ ion is not located. Finally, two additional benzoate groups, each bridging a Mn^{II}/Mn^{III} pair, complete the ligation, making Mn1 six coordinate and Mn2 seven coordinate. Mn1 and Mn1′ display JT elongations along the O4-Mn1-N1 and O4′-Mn1′-N1′ axes.

Solid-state DC magnetic susceptibility (χ_M) measurements were made on **1** and **2** in a 0.1 tesla field in the 5.00–300 K range. The obtained data are shown as $\chi_M T$ versus T plots in Figure 2, and indicate that both **1** and **2** have relatively large ground-state spin values. These values were determined by fits of magnetization (M) data collected in the 1.8–10 K and 0.1–3 T ranges: the fits are shown in Figure 3, and the fit parameters were $S=7$, $g=1.91$, and $D=-0.37$ K for **1**, and $S=9$, $g=1.78$, and $D=-0.22$ K for **2**. When data collected at fields higher than 3 T were used, the fits were poor, suggesting the presence of low-lying excited states, as expected for species containing Mn^{II} ions, which give weak exchange interactions. The use of low-field data to avoid this common problem has been described elsewhere.[10,11] The $S=9$ ground state of **2** is as expected for all the exchange interactions in the cluster being ferromagnetic, as found in other compounds with a related core.[5] The $S=7$ ground state of **1**, however, is most unusual for an Mn^{II}_6,Mn^{III}_6 species.

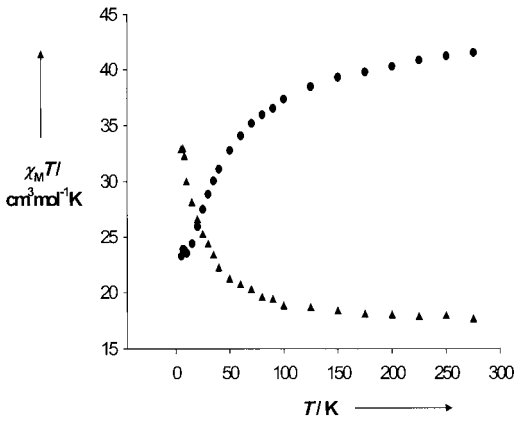

Figure 2. $\chi_M T$ versus T plots for complexes **1** (●) and **2** (▼).

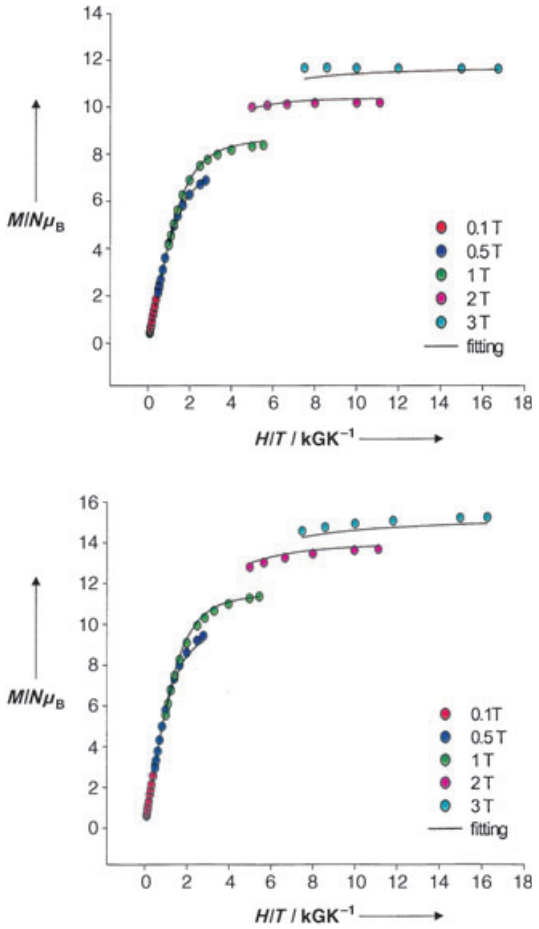

Figure 3. Magnetization (M) versus field (H) and temperature (T) data, plotted as reduced magnetization ($M/N\mu_B$) versus H/T, for complexes **1** (top) and **2** (bottom) at applied fields of 0.1, 0.5, 1.0, 2.0 and 3.0 T and in the 1.8 to 10 K temperature range. The solid lines are the fits of the data; see the text for the fit parameters.

Since **1** and **2** have significant ground-state S values, AC susceptibility measurements were performed in the 1.8–10 K range with a 3.5 G AC field oscillating at 50–1500 Hz to determine if they might be SMMs. Indeed, frequency-dependent tails were seen of out-of-phase (χ_M'') signals whose maxima lie below the operating minimum temperature of our SQUID instrument (1.8 K). In addition, the in-phase (χ_M') signals support the S values obtained for **1** and **2** from the above magnetization fits. Confirmation that **1** and **2** are SMMs was obtained from magnetization (M) versus applied DC field scans on single crystals down to 0.04 K, these scans displayed hysteresis, the diagnostic property of a magnet (Figure 4). The hysteresis loops for **1** show the characteristic steps arising from quantum tunneling of the magnetization (QTM), with the step sizes increasing with decreasing scan rates, as expected for SMMs. The loops for **2** are similar, but

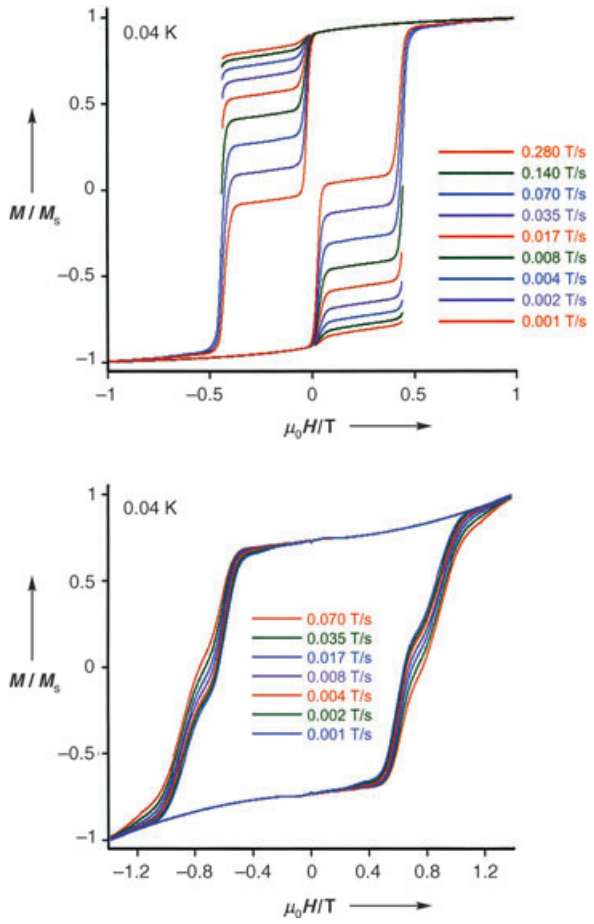

Figure 4. Magnetization (*M*) versus field (*H*) hysteresis loops for complexes **1** (top) and **2** (bottom) at 0.04 K and at the indicated scan rates; the magnetization is normalized to its saturation value (M_S).

have an unusual background slope owing to the presence of two molecules with different orientations in the unit cell. The field was applied along the easy axis (*z* axis) of one molecule and thus approximately transverse to the easy axis of the other; these field orientations should give a step-like hysteresis loop and a linear slope from the two molecules, respectively, and a combination of the two results is thus observed. Complex **1** is a rare example of a SMM with a single-strand loop structure, with only a Mn_{16} complex with $S = 10$[1a] and a Ni_{12} complex with $S = 12$[12] being reported to date.

Magnetization decay studies were carried out at different temperatures, and the resulting relaxation time (τ) versus T data used to construct τ versus $1/T$ Arrhenius plots. The effective barriers to relaxation (U_{eff}) can be obtained from the slopes in the thermally activated regions and the pre-exponential factors (τ_0) from the intercepts. These were $U_{eff} = 11$ K and $\tau_0 = 7 \times 10^{-7}$ s for **1**, and $U_{eff} = 15.3$ K and $\tau_0 = 3 \times 10^{-7}$ s for **2**. At very low temperatures, both compounds display the temperature-independent relaxation characteristic of QTM.

The $S = 7$ ground state of **1** is unusually intermediate in magnitude for a single-stranded Mn^{II}_6,Mn^{III}_6 loop complex: antiferromagnetic or ferromagnetic Mn^{II}/Mn^{III} exchange interactions would be expected to give $S = 3$ or 27 ground states, respectively, so it is clear that there must be both types of interaction within low-symmetry **1**. Since a quantitative rationalization of the *S* values of low-symmetry, high-nuclearity clusters is rarely available, and yet is crucial to our full understanding of their magnetic properties, we have carried out DFT calculations on **1**.

The entire complex is too large to be considered with DFT, so several smaller model clusters were constructed; a similar approach has been used by others for a number of complexes.[13] The six symmetry-inequivalent Mn ions were divided into two clusters of three, the first including Mn3, Mn4, and Mn5 and the second including Mn2, Mn1, and Mn6′. In defining the model clusters, ligands bridging metal centers had to be made terminal. To do so, carboxylate ligands were protonated to give $MeCO_2H$ ligands, with the H^+ ion added outside the cluster at a distance of 1.0 Å along the line connecting the O atom and the metal. Only the oxygen-donor site was retained for mda^{2-} ligands bridging between the different clusters, along with the first carbon atom of the corresponding ethylene chain. The second carbon atom was replaced with a hydrogen atom at a bond length scaled to 1.1 Å, giving an MeO^- ligand. In this way, the model clusters had neutral charge, as does the parent complex, and a reasonable simulation of the ligand field of each Mn was maintained.

With the above-described alterations, Mn3, Mn4, and Mn5 are included in the model complex $[Mn^{II}Mn^{III}_2(O_2CMe)_2(HO_2CMe)_2(mda)_3]$. Similarly, Mn2, Mn1, and Mn6′ are included in the model complex $[Mn^{II}_2Mn^{III}(O_2CMe)_3(HO_2CMe)_4(OMe)_2(mda)]$. Finally, the connections between the units, Mn2–Mn3 and Mn5–Mn6, are each modeled with the dinuclear complex $[Mn^{II}Mn^{III}(O_2CMe)(HO_2CMe)_3(OMe)_2(mda)]$; although this formula is identical for both connections, the structural parameters are not, and retain the same values as those in the Mn2–Mn3 and Mn5–Mn6 subunits of complex **1**.

Atomic spin densities were monitored in the calculations to ensure the correct spin components were obtained for each cluster. Values of 4.77, 3.71, and 3.71 were obtained for the high-spin component of the $Mn^{II}Mn^{III}_2$ cluster, for example. The energies of these components were then used to find the exchange parameters (Table 1). It is clear that all the *J* values are weak, in the range $4.0 > J > -4.6$ cm^{-1}. This range is fully consistent with values for $Mn^{II}Mn^{III}$ exchange parameters,

Table 1: Exchange parameters (*J*), using the $\hat{\mathcal{H}} = -2J\hat{S}_i\hat{S}_j$ convention, from DFT calculations on complex **1**.

Interactions	*J*
Mn4–Mn5, Mn4′–Mn5′[a]	+4.0
Mn3–Mn4, Mn3′–Mn4′[a]	+3.5
Mn2–Mn3, Mn2′–Mn3′[b]	−4.6
Mn5–Mn6, Mn5′–Mn6′[b]	−2.5
Mn1–Mn2, Mn1′–Mn2′[c]	−1.4
Mn1–Mn6′, Mn1′–Mn6[c]	+0.0[d]

[a] Model complex $[Mn^{II}Mn^{III}_2(O_2CMe)_2(HO_2CMe)_2(mda)_3]$. [b] Model complex $[Mn^{II}Mn^{III}(O_2CMe)(HO_2CMe)_3(OMe)_2(mda)]$. [c] Model complex $[Mn^{II}_2Mn^{III}(O_2CMe)_3(HO_2CMe)_4(OMe)_2(mda)]$. [d] Small ferromagnetic value (+0.02 cm^{-1}) calculated for this parameter.

which are always weak and either side of zero, depending on the bridges.[14] The ferromagnetic ($J > 0$) parameters correspond to Mn_2 pairs bridged by two mono-atomic alkoxide bridges, whereas all the other bridging types are antiferromagnetic; this is the same pattern as in dinuclear $Mn^{II}Mn^{III}$ complexes.[14] Within the uncertainty of the DFT calculation, the Mn1–Mn6′ and Mn1′–Mn6 interactions are calculated to be 0.0 cm^{-1}: in fact, they are almost certainly either very weakly positive or negative. Since the spin of each half of the molecule is calculated to be $S = 7/2$, positive Mn1–Mn6′ and Mn1′–Mn6 interactions would give a ground-state spin of $S = 0$ while negative Mn1–Mn6′ and Mn1′–Mn6 interactions give $S = 7$, for the complete molecule (Figure 5). On the basis of

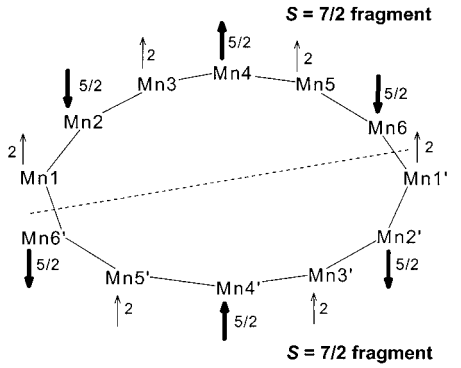

Figure 5. Depiction of the spin alignments in the $S = 7$ ground state of complex **1** as predicted by the DFT calculations, with the Mn1–Mn6′ and Mn1′–Mn6 interactions antiferromagnetic. The Mn labeling scheme is the same as that in Figure 1 (top). The dashed line separates the two $S = 7/2$ fragments that are coupled by the interactions between Mn1–Mn6′ and Mn1′–Mn6; if these interactions are antiferromagnetic (negative J values), the resultant spin of the complete molecule is $S = 7$.

the magnetization data described above, complex **1** clearly does not have an $S = 0$ ground state, and we thus conclude that the ground state is $S = 7$, resulting from the spin alignments in Figure 5. Weakly antiferromagnetic Mn1–Mn6′ and Mn1′–Mn6 interactions are in fact consistent with the nature of the bridging ligands at these sites.[14] The conclusion that $S = 7$ is also in complete agreement with the magnetization fits and in-phase AC data.

In summary, the use of $mdaH_2$ has led to new Mn_{12} and Mn_4 SMMs with $S = 7$ and $S = 9$ ground-state spins, respectively. The Mn_{12} species is a very rare example of a SMM with a loop structure,[1a,21] and its unusual $S = 7$ ground state for an $Mn^{III}_6Mn^{II}_6$ species has been rationalized by DFT calculations to be due to the variety of exchange interactions present.

Experimental Section

1·MeCN: Method A: $mdaH_2$ (0.23 mL, 1.0 mmol) and NEt_3 (0.28 mL, 1.0 mmol) were added to a stirred solution of $Mn(O_2CMe)_2{\cdot}4H_2O$ (0.50 g, 1.0 mmol) in MeCN (30 mL), which caused a rapid color change to dark brown. The resulting dark brown solution was stirred for 1 h, and then layered with diethyl ether. After several days, dark red crystals of **1**·MeCN were collected by filtration, washed with Et_2O (2×15 mL), and dried in air. The yield was 55%. Elemental analysis (%) calcd for $C_{72}H_{136}Mn_{12}N_{10}O_{44}$ (**1**·MeCN): C 33.92, H 5.42, N 4.87; found: C 34.33, H 5.72, N 4.48.

Method B: $mdaH_2$ (0.29 mL, 1.0 mmol), NaO_2CMe_2 (0.42 g, 2.0 mmol) and NEt_3 (0.35 mL, 1.0 mmol) were added to a stirred solution of $MnCl_2{\cdot}4H_2O$ (0.50 g, 1.0 mmol) in MeCN (30 mL), which caused a rapid color change to dark brown. The resulting dark brown solution was stirred for 1 h and then layered with diethyl ether. After several days, dark red crystals of **1**·MeCN were collected by filtration, washed with ether and dried in air; yield 46%. The material was spectroscopically identical with the material from Method A.

2·CH_2Cl_2·Et_2O: $mdaH_2$ (0.17 g, 1.0 mmol) was added to a stirred solution of $Mn(O_2CPh)_2{\cdot}4H_2O$ (0.50 g, 1.0 mmol) in MeCN (30 mL) and NEt_3 (0.21 mL, 1.0 mmol), which caused a rapid color change to dark brown. The resulting dark brown solution was stirred for 1 h and the resulting precipitate was collected by filtration, washed with MeCN, dissolved in CH_2Cl_2 (50 mL), filtered, and the filtrate layered with diethyl ether. After several days, light brown crystals of **2** were collected by filtration, washed with diethyl ether (2×15 mL), and dried in air; yield 16%. Elemental analysis (%) calcd for $C_{58}H_{90}Cl_4Mn_4N_4O_{18}$ (**2**·CH_2Cl_2·Et_2O): C 48.99, H 5.82, N 4.76; found: C 48.99, H 5.44, N 4.56.

Density functional theory (DFT) calculations were carried out using the B3LYP functional[15] implemented in the Gaussian 98 program,[16] with the all-electron Dunning–Huzinaga double-ζ basis for light atoms[17] and the Los Alamos effective core potential plus double-ζ valence basis set for manganese atoms.[18] The procedure given in ref. [19] was used to obtain starting orbitals for the DFT calculations. The exchange constants were found by fitting calculated energies and spin couplings to the Heisenberg Hamiltonian.[19,20]

Received: August 29, 2004
Published online: December 28, 2004

Keywords: cluster compounds · density functional calculations · magnetic properties · manganese · single-molecule magnets

[1] a) M. Murugesu, W. Wernsdorfer, K. A. Abboud, G. Christou, *Angew. Chem.* **2005**, *117*, 914; *Angew. Chem. Int. Ed.* **2005**, *44*, 892; b) A. J. Tasiopoulos, W. Wernsdorfer, K. A. Abboud, G. Christou, *Angew. Chem.* **2004**, *116*, 6498; *Angew. Chem. Int. Ed.* **2004**, *43*, 6338; c) G. Christou, D. Gatteschi, D. N. Hendrickson, R. Sessoli, *MRS Bull.* **2000**, *25*, 66; d) R. Sessoli, H.-L. Tsai, A. R. Schake, S. Wang, J. B. Vincent, K. Folting, D. Gatteschi, G. Christou, D. N. Hendrickson, *J. Am. Chem. Soc.* **1993**, *115*, 1804; e) R. Sessoli, D. Gatteschi, A. Caneschi, M. A. Novak, *Nature* **1993**, *365*, 141.

[2] F. D. Rochon, A. L. Beauchamp, C. C. Bensimon, *Can. J. Chem.* **1996**, *74*, 2121.

[3] F. D. Rochon, R. Melanson, P. C. Kong, *Inorg. Chim. Acta* **1997**, 254, 303.

[4] J. M. Berg, R. H. Holm, *Inorg. Chem.* **1983**, *22*, 1768.

[5] a) E. K. Brechin, J. Yoo, M. Nakano, J. C. Huffman, D. N. Hendrickson, G. Christou, *Chem. Commun.* **1999**, 783–784; b) J. Yoo, E. K. Brechin, A. Yamaguchi, M. Nakano, J. C. Huffman, A. L. Maniero, L.-C. Brunel, K. Awaga, H. Ishimoto, G. Christou, D. N. Hendrickson, *Inorg. Chem.* **2000**, *39*, 3615.

[6] C. Boskovic, W. Wernsdorfer, K. Folting, J. C. Huffman, D. N. Hendrickson, G. Christou, *Inorg. Chem.* **2002**, *41*, 5107.

[7] M. Murugesu, M. Habrych, W. Wernsdorfer, K. A. Abboud, G. Christou, *J. Am. Chem. Soc.* **2004**, *126*, 4766.

[8] Crystal structure data for **1**·MeCN: $C_{72}H_{136}Mn_{12}N_{10}O_{44}$, $M_r = 2505.19$, triclinic, space group $P\bar{1}$, $a = 13.1062(13)$, $b = 13.2707(13)$, $c = 17.2424(17)$ Å, $\alpha = 107.223(2)$, $\beta = 109.214(2)$, $\gamma = 99.260(2)°$, $V = 2591.6(4)$ Å^3, $T = 100(2)$ K, $Z = 2$, $\rho_{calcd} = 1.605$ g cm^{-3}, 17243 reflections collected, 8624 unique ($R_{av} = 0.0868$), $R1 = 0.0486$, w$R2 = 0.0891$, using 5470 reflections with

$I > 2\sigma(I)$. Crystal structure data for **2**·CH_2Cl_2·Et_2O: $C_{58}H_{90}Cl_4Mn_4N_4O_{18}$, $M_r = 1492.90$, Monoclinic, space group $P2_1/n$, $a = 18.069(2)$, $b = 8.3713(11)$, $c = 23.707(3)$ Å, $\alpha = 90°$, $\beta = 102.096(3)$, $\gamma = 90°$, $V = 3506.3(8)$ Å^3, $T = 173$ K, $Z = 1$, $\rho_{calcd} = 1.414$ g cm^{-3}, 18497 reflections collected, 8624 unique ($R_{av} = 0.0868$), $R1 = 0.0718$, w$R2 = 0.1839$, using 18497 reflections with $I > 2\sigma(I)$. CCDC-248525 and CCDC-248526 contain the supplementary crystallographic data for this paper. These data can be obtained free of charge via www.ccdc.cam.ac.uk/conts/retrieving.html (or from the Cambridge Crystallographic Data Centre, 12 Union Road, Cambridge CB21EZ, UK; fax: (+44) 1223-336-033; or deposit@ccdc.cam.ac.uk).

[9] a) Bond valence sum (BVS) calculations for the Mn ions of **1** gave values of 2.83 (for Mn1), 1.90 (Mn2), 2.95 (Mn3), 1.74 (Mn4), 2.96 (Mn5) and 1.83 (Mn6), and for the Mn ions of **2** gave values of 3.01 (for Mn1) and 1.86 (Mn2); b) W. Liu, H. H. Thorp, *Inorg. Chem.* **1993**, *32*, 4102; c) Brown, I. D. Altermatt, *Acta Crystallogr. Sect. B* **1985**, 244.

[10] M. Soler, W. Wernsdorfer, K. Folting, M. Pink, G. Christou, *J. Am. Chem. Soc.* **2004**, *126*, 2156–2165.

[11] E. C. Sañudo, W. Wernsdorfer, K. A. Abboud, G. Christou, *Inorg. Chem.* **2004**, *43*, 4137.

[12] C. Cadiou, M. Murrie, C. Paulsen, V. Villar, W. Wernsdorfer, R. E. P. Winpenny, *Chem. Commun.* **2001**, 2666.

[13] a) J. Cano, P. Alemany, S. Alvarez, M. Verdaguer, E. Ruiz, *Chem. Eur. J.* **1998**, *4*, 476; b) E. Ruiz, J. Cano, S. Alvarez, P. Alemany, *J. Am. Chem. Soc.* **1998**, *120*, 11122; c) E. Ruiz, J. Cano, S. Alvarez, P. Alemany, *J. Comput. Chem.* **1999**, *20*, 1391; d) E. Ruiz, A. Rodriguez-Fortea, J. Cano, S. Alvarez, *J. Comput. Chem.* **2003**, *24*, 982; e) R. Carrasco, J. Cano, T. Mallah, L. F. Jones, D. Collison, E. K. Brechin, *Inorg. Chem.* **2004**, *43*, 5410.

[14] L. Que, A. E. True, *Prog. Inorg. Chem.* **1990**, *38*, 97.

[15] A. D. Becke, *J. Chem. Phys.* **1993**, *98*, 5648; C. Lee, W. Yang, R. G. Parr, *Phys. Rev. B* **1988**, *37*, 785.

[16] Gaussian 98 (Revision A.7), M. J. Frisch, G. W. Trucks, H. B. Schlegel, G. E. Scuseria, M. A. Robb, J. R. Cheeseman, V. G. Zakrzewski, J. A. Montgomery, R. E. Stratmann, J. C. Burant, S. Dapprich, J. M. Millam, A. D. Daniels, K. N. Kudin, M. C. Strain, O. Farkas, J. Tomasi, V. Barone, M. Cossi, R. Cammi, B. Mennucci, C. Pomelli, C. Adamo, S. Clifford, J. Ochterski, G. A. Petersson, P. Y. Ayala, Q. Cui, K. Morokuma, D. K. Malick, A. D. Rabuck, K. Raghavachari, J. B. Foresman, J. Cioslowski, J. V. Ortiz, B. B. Stefanov, G. Liu, A. Liashenko, P. Piskorz, I. Komaromi, R. Gomperts, R. L. Martin, D. J. Fox, T. Keith, M. A. Al-Laham, C. Y. Peng, A. Nanayakkara, C. Gonzalez, M. Challacombe, P. M. W. Gill, B. G. Johnson, W. Chen, M. W. Wong, J. L. Andres, M. Head-Gordon, E. S. Replogle, J. A. Pople, Gaussian, Inc., Pittsburgh, PA, **1998**..

[17] T. H. Dunning, P. J. Hay in *Modern Theoretical Chemistry* (Ed.: H. F. Schaefer III), Plenum, New York, **1976**, 1–28.

[18] P. J. Hay, W. R. Wadt, *J. Chem. Phys.* **1985**, *82*, 270.

[19] E. R. Davidson, A. E. Clark, *J. Phys. Chem. A* **2002**, *106*, 7456.

[20] T. A. O'Brien, E. R. Davidson, *Int. J. Quantum Chem.* **2003**, *92*, 294.

[21] Note added in proof (December 13, 2004): Complex **1** has recently been reported by others: E. M. Rumberger, L. N. Zakharov, A. L. Rheingold, D. N. Hendrickson, *Inorg. Chem.* **2004**, *43*, 6531.

